

# Aufbau suppressed coupled cluster as a post-linear-response method

Trine Kay Quady,<sup>1</sup> Harrison Tuckman,<sup>1</sup> and Eric Neuscamman<sup>1,2</sup>

<sup>1</sup>*Department of Chemistry, University of California, Berkeley, California 94720, USA*

<sup>2</sup>*Chemical Sciences Division, Lawrence Berkeley National Laboratory, Berkeley, California 94720, USA*

(\*Electronic mail: eneuscamman@berkeley.edu)

(Dated: 23 June 2025)

We investigate the ability of Aufbau suppressed coupled cluster theory to act as a post-linear-response correction to widely used linear response methods for electronically excited states. We find that the theory is highly resilient to shortcomings in the underlying linear response method, with final results from less accurate starting points nearly as good as those from the best starting points. This pattern is especially stark in charge transfer states, where the approach converts starting points with multi-eV errors into post-linear-response results with errors on the order of 0.1 eV. These findings highlight the ability of Aufbau suppressed coupled cluster to perform its own orbital relaxations and raise the question of whether initializing it with an orbital relaxed reference is worth the trouble.

## I. INTRODUCTION

Capturing post-excitation relaxations in a molecule’s molecular orbitals (MOs) is often critical for making accurate excited state predictions. Indeed, recent examples from configuration interaction (CI),<sup>1–3</sup> density functional theory (DFT),<sup>4–6</sup> and multi-reference methods<sup>7–10</sup> provide clear demonstrations of how excited-state-specific MO optimizations can improve on the partial MO relaxations achieved through linear response methods. While these results are encouraging, they are also somewhat frustrating, because the convenience of getting many states out of a single linear-response-style diagonalization gets replaced by state-by-state nonlinear MO optimizations. Noting that ground state coupled cluster (CC) theory<sup>11–13</sup> can be remarkably insensitive to the initial choice of MO basis,<sup>14–16</sup> one might wonder whether something similar is true for the Aufbau suppressed CC (ASCC) approach<sup>17–19</sup> to excited states. After all, both methods can perform their own orbital relaxations via the CC singles operator,<sup>20</sup> and so it may be that ASCC, if initiated from the results of widely used linear response methods, could combine linear response’s ease of use with the accuracy of state-specific MO relaxations. As our results demonstrate, ASCC is indeed quite insensitive to its starting point, allowing it to be used as a high-accuracy, post-linear-response refinement method in conjunction with CI singles (CIS),<sup>21</sup> time-dependent DFT (TD-DFT),<sup>22–24</sup> or equation of motion CC (EOM-CC).<sup>25–27</sup>

Excitations that involve substantial orbital relaxations pose challenges for many widely used excited state methods. Linear response approaches — such as EOM-CC with singles and doubles (EOM-CCSD), linear response CC,<sup>28–34</sup> and TD-DFT — are not able to fully account for these inherently nonlinear relaxations.<sup>35,36</sup> As a result, these methods display reduced accuracy for charge transfer (CT)<sup>37–42</sup> and core excitations.<sup>5,43,44</sup> Similarly, the widely used state averaging approach in complete active space self consistent field (CASSCF) theory — in which all states are forced to share the same MO basis — creates significant errors for CT states,<sup>7,8,45,46</sup> which require different orbital polarizations than the ground state and most other excited states. These dif-

ficulties are not just an issue for excitation energies: they can also produce large errors in the excited state potential energy surfaces<sup>8,47</sup> that control photochemical reactions.

Instead of relying on ground state or partially relaxed orbitals, an increasing number of approaches seek to fully relax the MOs in the presence of the excitation. These approaches include a number of DFT,<sup>4–6,48–62</sup> variational Monte Carlo,<sup>46,63–73</sup> CASSCF,<sup>7–9,74–76</sup> perturbation theory,<sup>47,77,78</sup> CC,<sup>79–84</sup> and CI methods.<sup>1–3,85–89</sup> In general, these excited-state-specific methods tend to be more accurate for CT and core excitations than their linear response counterparts, but this improved accuracy comes at a cost. Unlike linear response — in which a single, well-conditioned diagonalization yields many excited states at once — these state-specific methods must perform individual nonlinear MO optimizations for each excited state separately. Although such optimizations have proven effective in many cases, convergence to the correct root is not trivial,<sup>88</sup> and there are known cases where convergence has failed.<sup>78</sup> Ideally, it would be possible to combine the best of both worlds by pairing the ease of use of linear response with the high accuracy of state-specificity.

Although ASCC theory was initially motivated as a way to build a CC theory atop excited state mean field (ESMF) theory,<sup>17</sup> its ability to incorporate its own state-specific orbital relaxations via its singles operator raises the possibility of instead pairing it with starting points from linear response theory. The basic idea is that the linear response method, via its convenient diagonalization, can produce a qualitatively correct starting point that ASCC then improves upon. Of course, this approach may simply shift the nonlinear MO optimization challenge into the ASCC equations, but this difficulty should be mitigated by linear response methods that at least partially relax the orbitals. For example, while CIS and TD-DFT are only able to relax the shapes of the hole and particle orbitals, EOM-CCSD is able to capture limited relaxation effects for all orbitals via its CI doubles operator, which would presumably lessen the difficulty of finalizing these relaxations with ASCC. Thus, we hope to use ASCC as a post-linear-response method that benefits from linear response’s ease of use while delivering improved, state-specific accuracy.

To test this approach, we have paired ASCC with CIS, TD-

DFT, and EOM-CCSD and tested the pairings on 145 singlet excitations spanning valence, Rydberg, and CT excited states. As in our previous studies of ASCC, we benefit enormously from the high quality QUEST database<sup>90,91</sup> as well as the CT benchmark of Szalay and coworkers.<sup>41</sup> Remarkably, we find that even when ASCC is initiated from TD-DFT or CIS starting points whose CT excitation energy errors are larger than 2 eV, the final ASCC results are typically on par with those initiated from ESMF or EOM-CCSD. Although there does remain a (very) small accuracy advantage to starting from ESMF, the results we present below call into question whether going to the trouble of performing ESMF's nonlinear orbital optimization is worthwhile in conjunction with ASCC. For singly-excited singlet excitations at least, the data strongly suggest that the most productive use of ASCC may well be as a post-linear-response method.

## II. THEORY

### a. Setting up ASCC

Like many CC theories, ASCC is motivated by the strong formal properties offered by an ansatz in which exponentiated operators act on a single-determinant reference. These properties include systematic improvability, size consistency, size extensivity, and, for excitation energies, size intensivity. Unlike most CC approaches, the ASCC wave function includes both an excitation operator  $\hat{T}$  and a de-excitation operator  $\hat{S}^\dagger$ .

$$|\Psi_{\text{ASCC}}\rangle = e^{-\hat{S}^\dagger} e^{\hat{T}} |\phi_0\rangle = (1 + \hat{T} - \hat{S}^\dagger \hat{T} + \dots) |\phi_0\rangle \quad (1)$$

The key idea is that, when acted on the Aufbau determinant  $|\phi_0\rangle$ , the term  $\hat{S}^\dagger \hat{T}$  produces a second copy of that determinant via an excite-then-de-excite process. So long as the sign on that copy is negative, it can wholly or partially cancel the main Aufbau term in the expansion, thus producing a state in which the Aufbau determinant is absent or present with only a small coefficient. Like other CC theories, the working equations involve a similarity transformed Hamiltonian.

$$\bar{H} = e^{-\hat{T}} e^{\hat{S}^\dagger} \hat{H} e^{-\hat{S}^\dagger} e^{\hat{T}} \quad (2)$$

$$E_{\text{ASCC}} = \langle \phi_0 | \bar{H} | \phi_0 \rangle \quad (3)$$

$$0 = \langle \mu | \bar{H} | \Phi_0 \rangle \quad (4)$$

Here  $\mu$  stands for any of the excited determinants corresponding to the individual excitation operators placed in  $\hat{T}$ . Partially linearized ASCC (PLASCC) uses these same working equations, but with certain nonlinear diagrams neglected in a balancing effort motivated by perturbative analysis.<sup>18</sup>

To decide what to include in  $\hat{T}$ , we follow perturbative arguments that first require us to define the zeroth order pieces of the wave function. In practice, we start with an initial guess for the excited state (e.g., from CIS, TD-DFT, ESMF, or EOM-CCSD) and truncate it down to only its most significant configuration state functions (CSFs). We then define the zeroth order pieces of  $\hat{S}$  and  $\hat{T}$  so that, when truncated to zeroth order, the ASCC wave function matches the truncated initial

guess, which we call our starting point. In the simplest case, the starting point has just one CSF in which an electron has been promoted from the hole orbital  $h$  to the particle orbital  $p$ , which gives us a particularly simple zeroth order setup.<sup>17</sup>

$$\hat{S} = \hat{S}^{(0)} = \frac{1}{\sqrt{2}} \left( \hat{p}_\uparrow^\dagger \hat{h}_\uparrow + \hat{p}_\downarrow^\dagger \hat{h}_\downarrow \right) \quad (5)$$

$$\hat{T}^{(0)} = \hat{S} - \frac{1}{2} \hat{S}^2 \quad (6)$$

In cases where there are multiple CSFs in the truncated starting point, the zeroth order setup is more complicated,<sup>18</sup> but key characteristics are maintained. Specifically,  $\hat{S} = \hat{S}^{(0)}$  will only contain zeroth order pieces, it will be a one-body operator, and it will only excite to and from orbitals that are half-occupied in at least one of the starting point CSFs.

With the zeroth order wave function chosen, we then define a suitable Hamiltonian partitioning<sup>18</sup> and flesh out  $\hat{T}$  by incorporating all excitation operators whose amplitudes appear at first order in perturbation theory. In the one-CSF case, this approach leads to including all singles and doubles excitations, as well as a small subset of triples (in multi-CSF cases, there are also small subsets of higher excitations). So long as there are only  $O(1)$  primary CSFs, the approach will have CCSD's  $O(N^6)$  cost scaling and contain only  $O(N^3)$  amplitudes beyond the doubles,<sup>18</sup> which clearly motivates us to seek compact starting points whose wave functions are dominated by a small number of CSFs. As we will now discuss, ESMF is far from the only way to get such starting points, as they are also readily available from a variety of different linear response theories.

### b. Starting from CIS

The CIS wave function is defined by its coefficient matrix  $C$ , which can be indexed by an occupied index  $i$  and virtual index  $a$ .

$$|\Psi_{\text{CIS}}\rangle = \sum_{ia} C_{ia} |\phi_i^a\rangle \quad (7)$$

Here  $|\phi_i^a\rangle$  is the singly-excited singlet CSF in which an electron has been excited from orbital  $i$  to orbital  $a$ . As shown by Martin,<sup>92</sup> the natural transition orbitals (NTOs) for CIS are derived from a singular value decomposition (SVD) of the matrix  $C$ , as  $C$  is also the CIS transition density matrix (TDM). If we work in this NTO basis, the wave function becomes

$$|\Psi_{\text{CIS}}\rangle = \sum_k \sigma_k |\phi_k^{\tilde{k}}\rangle, \quad (8)$$

where  $k$  and  $\tilde{k}$  label the occupied NTO and virtual NTO corresponding to singular value  $\sigma_k$ . As a truncated SVD is (in the least-squares sense) the best low-rank approximation of a matrix,<sup>93</sup> we produce an optimal truncation of the CIS state for our ASCC starting point by moving into the CIS NTO basis, dropping small singular values (we use a threshold of 0.2), and renormalizing.

### c. Starting from ESMF

For ESMF, we will again prepare the ASCC starting point via a truncated SVD approach, but, due to ESMF’s orbital relaxations, the matrix in question is not the ESMF TDM. We start in the relaxed ESMF orbital basis, in which the ESMF state takes the same form as Eq. (7).<sup>3</sup> From there, we follow the same procedure of taking the SVD of the ESMF  $C$  matrix and using the singular vectors to rotate to an MO basis in which the CI matrix becomes diagonal, as in Eq. (8). Since the ESMF MOs differ from the ground state Hartree Fock MOs,  $C$  is not the ESMF TDM, and so this new basis resulting from an SVD of  $C$  is not the NTO basis. We have therefore instead referred to it as ESMF’s transition orbital pair (TOP) basis when employing it in other post-ESMF methods.<sup>77</sup> Nonetheless, the ESMF TOP basis is a close cousin to the CIS NTO basis, and it will play the same role in our ASCC starting point preparation. After moving to the TOP basis, we truncate small singular values and renormalize to produce our starting point.

### d. Starting from EOM-CCSD

The nature of the EOM-CCSD TDM creates complications for our approach. To start, there are actually two different TDMs that appear in the theory,<sup>26</sup> owing the fact that the left and right eigenvectors of its non-Hermitian similarity transformed Hamiltonian are not the same. Further, correlation effects prevent either of these TDMs from having the simple occupied-by-virtual rectangular structure of the CIS TDM, which in turn means that their singular vectors do not define a change of MO basis that keeps occupieds and virtuals separate. In a state where the TDM has just one singular value significantly different than zero, the other singular vectors can strongly mix occupied and virtual orbitals with each other, creating an MO basis that is difficult to interpret and poorly suited for a theory that intends to define  $\hat{T}$  as being built from operators that, roughly speaking, excite from the occupied space to the virtual space.

To overcome these challenges, we define our EOM-CCSD-based ASCC starting point using a combination of the “right-hand”  $\langle L_{\text{ground}} | \cdots | R_{\text{excited}} \rangle$  EOM-CCSD TDM<sup>26</sup> and the EOM-CCSD excited state natural orbitals (NOs). We start by performing an SVD of the TDM and identifying above-threshold singular values. We then form a list of (not yet orthogonal) occupied orbitals that begins with the above-threshold left hand singular vectors in descending order, followed by the natural orbitals with occupations near two. We form a second list of (not yet orthogonal) virtual orbitals from the above-threshold right hand singular vectors, followed by the natural orbitals with occupations close to zero. Note that the natural orbitals corresponding to the retained left and right singular vectors (those with the largest overlaps) are not used. Finally, we combine these lists by interleaving them — occupied, virtual, occupied, virtual, etc — and then performing a Gram–Schmidt process to arrive at an orthonormal MO basis. As in Eq. (8), our starting point is then built from the CSFs corresponding to the above-threshold singular values.

### e. Starting from TD-DFT

Although practical implementations of TD-DFT tend to lead to TDMs with nonzero entries only in the occupied-virtual and (if not using Tamm-Dancoff) virtual-occupied blocks<sup>94</sup> and so will yield NTOs that do not mix occupieds with virtuals, exact TD-DFT would match full CI which, like EOM-CCSD, can mix occupieds and virtuals in its NTOs. We therefore choose to prepare our truncated TD-DFT starting point in the same manner as for EOM-CCSD. Specifically, we have employed the Tamm-Dancoff TDM and excited state NOs in the same manner as we employed the EOM-CCSD TDM and excited state NOs above. In tests, we have verified that this approach leads to excitation energies that are virtually indistinguishable (within 0.01 eV) from the alternative option of preparing the starting point via the CIS approach with the Tamm-Dancoff TDM swapped in for the CIS TDM.

## III. RESULTS

### a. Computational Details

CIS, ESMF, TD-DFT, and EOM-CCSD vertical excitation energies, and their corresponding ASCCSD and PLASCCSD counterparts, were compared against benchmark results from three datasets containing singly excited valence, Rydberg, and charge transfer states. CIS calculations were performed with PySCF<sup>95</sup> while EOM-CCSD and TD-DFT/ $\omega$ B97X-V<sup>96</sup> calculations were performed using Q-Chem 6.2.<sup>97</sup> The TDMs and NOs used to derive ASCC starting points from EOM-CCSD and (TDA) TD-DFT were produced by Q-Chem’s excited state analysis module.

The benchmark results include the QUEST small and medium molecular benchmark datasets,<sup>90,91</sup> which together contain 188 single excitations, including singlet valence and Rydberg excited states, while the remaining dataset consists of seven charge transfer states.<sup>18</sup> In this work and in the benchmarks, valence and Rydberg calculations were performed in the aug-cc-pVDZ basis while charge transfer calculations were performed in the cc-pVDZ basis. While the benchmark sets used the frozen core approximation and the present calculations did not, freezing the core typically has a 0.02 eV or smaller effect on the excitation energy<sup>90,91</sup> and so does little to interfere with the comparisons.

In prior work,<sup>18</sup> the 188 states from the two QUEST sets were filtered down to 144 states by focusing on one- and two-CSF singly excited states, excluding a handful of cases that lacked ESMF, ASCC, or PLASCC solutions, and excluding two-CSF states in molecules too large for our pilot two-CSF implementation to handle. In the present study, different starting points prove to be better and worse for different states, and in a number of cases one or more of the new starting points was poor enough that ASCC or PLASCC failed to converge, even though they had converged when starting from ESMF. Some starting points also proved to have more than two CSFs, which is beyond the capabilities of our current ASCC code base. In order to focus on cases where a comparison across at

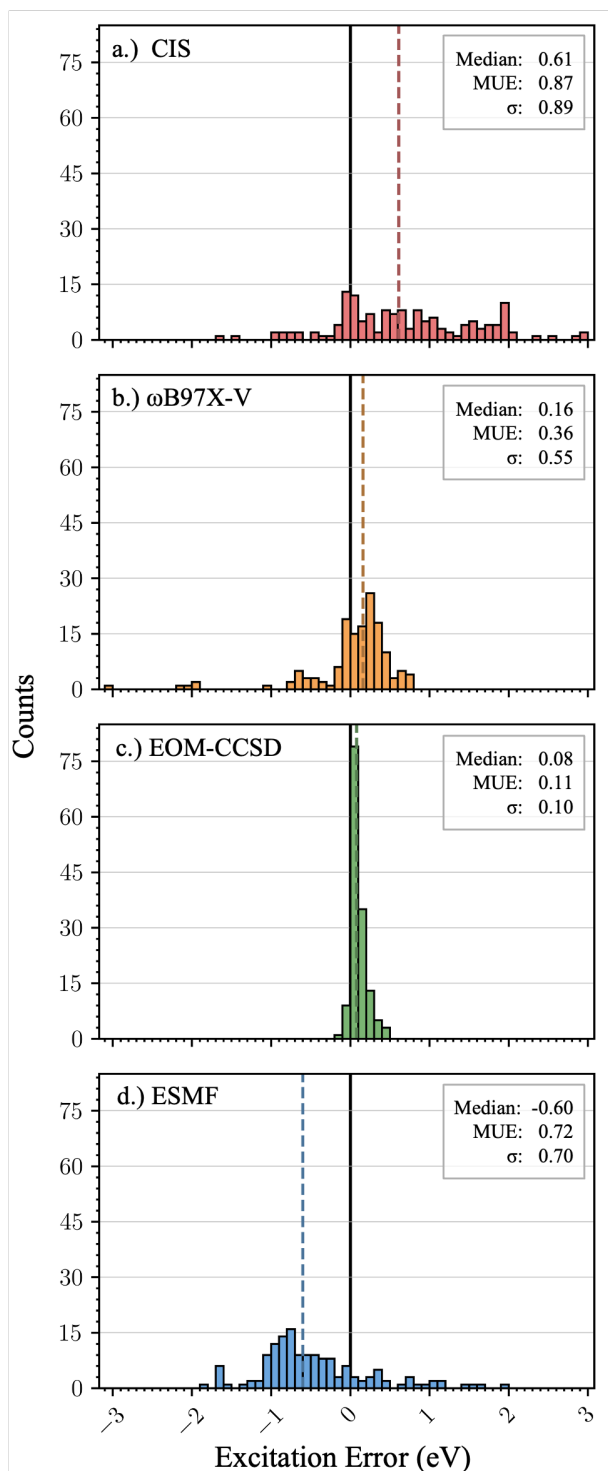


FIG. 1. Distributions of excitation energy errors for CIS, TD-DFT/ $\omega$ B97X-V, EOM-CCSD, and ESMF across all states, which include the seven charge transfer states and all states in our reduced test set of singlet valence and Rydberg excitations. The dashed line shows a method's median error, while the insets report this median, the mean unsigned error (MUE), and the standard deviation ( $\sigma$ ).

least three starting points was possible, we have therefore also excluded states where two or more of the starting points failed to converge or had more than two large CSFs. This winnowing leaves us considering a reduced test set of 138 valence and Rydberg excitations (see SI for details). In addition, we consider all seven charge transfer states from and use the the same convergence criteria and two-ansatz averaging procedure from the recent perturbative analysis study.<sup>18</sup>

## b. Starting method energies

To appreciate the degree to which ASCC and PLASCC are able to offer improvement over different starting points, we first analyze the accuracy of the starting point methods themselves. As seen in Figure 1, EOM-CCSD is by far the most accurate, with TD-DFT/ $\omega$ B97X-V showing intermediate accuracy. Both CIS and ESMF show relatively poor accuracy, but in interestingly different ways. Lacking orbital relaxations, CIS tends to error high.<sup>21</sup> In contrast, ESMF tends to error low, which can be explained by the fact that, while it lacks most correlation effects, it does capture the strong correlation between the two electrons involved in the excitation's open-shell singlet. The ground state energy from Hartree Fock that is used to get the ESMF excitation energy difference lacks all correlation effects, and so we would expect ESMF to on average error low by about one electron pair's worth of correlation, which is roughly what we see.

Although they are in some cases hidden in the distribution, the charge transfer states prove especially challenging for the four starting methods. In CIS and EOM-CCSD, they produce errors at the high end of the error distribution, whereas in TD-DFT they produce large negative errors that stand out clearly on the left hand side of its error distribution. Given EOM-CCSD's especially high accuracy for valence and Rydberg states, we would expect the largest improvements from subsequent ASCC and PLASCC improvements to occur for the charge transfer states. Based on the accuracy reached in previous studies, we would hope that ASCC and especially PLASCC could make significant improvements on the other three starting points in all three categories of states: valence, Rydberg, and charge transfer. We will begin with the first two categories, after which we will turn our attention to the especially challenging case of charge transfer.

## c. Valence and Rydberg states

Remarkably, when we apply ASCC and PLASCC to the ESMF, CIS, TD-DFT, and EOM-CCSD starting points, the resulting accuracies are quite similar and amount to a significant improvement over three of the four starting methods. As seen in Figure 2, the median error and mean unsigned error (MUE) for ASCC is quite insensitive to the starting point used. A similar result occurs for PLASCC, which also proves again to be more accurate than ASCC. In PLASCC, we also see a small accuracy advantage when starting from EOM-CCSD and especially ESMF, which we presume is thanks to the fact that

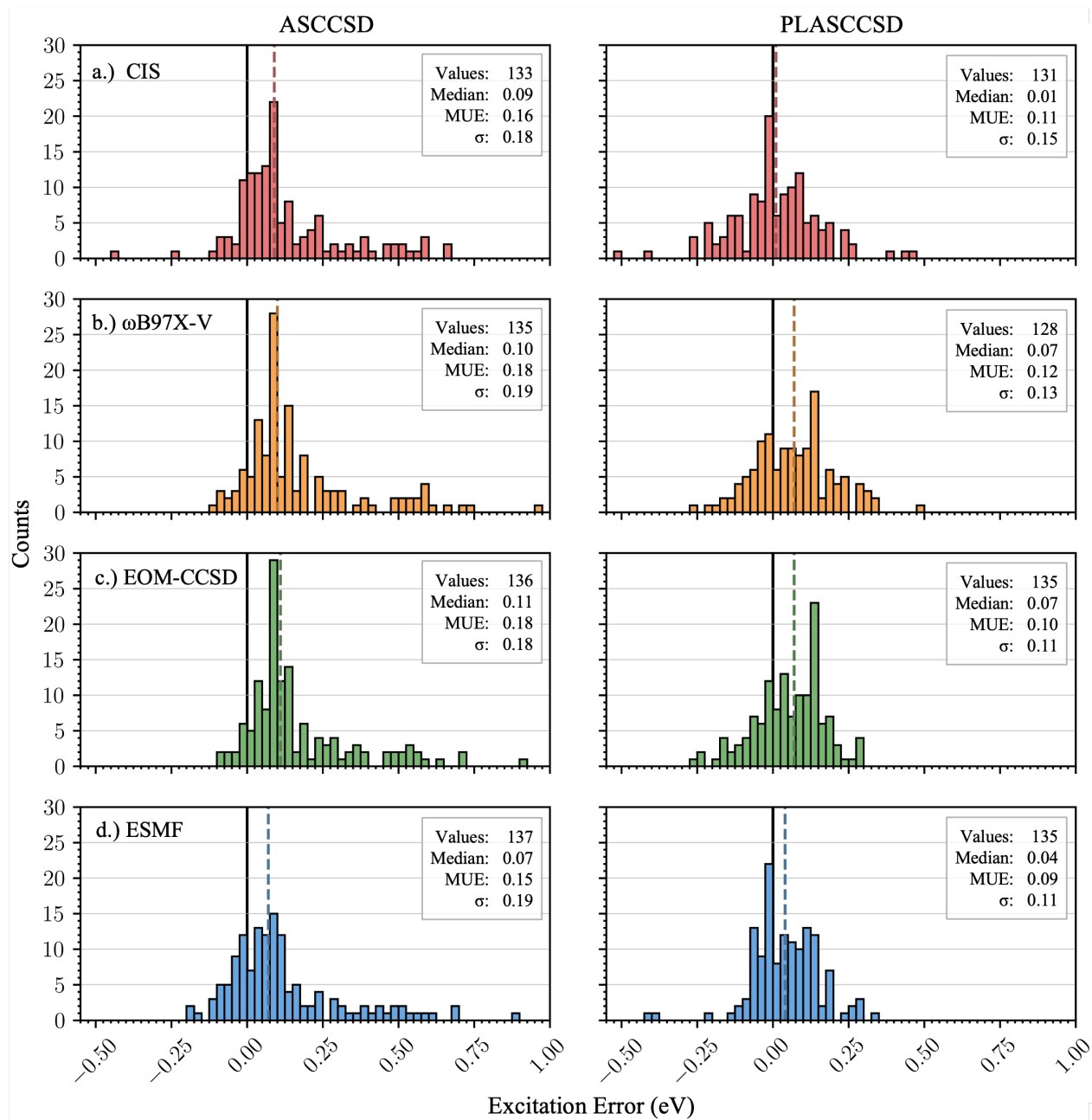


FIG. 2. Excitation energy error distributions for ASCCSD (left) and PLASCCSD (right) on our reduced test set of valence and Rydberg excitations. From top to bottom, the starting points used were CIS,  $\omega$ B97X-V, EOM-CCSD, and ESMF. The dashed lines show the median errors, while the insets report these, the mean unsigned error (MUE), the standard deviation ( $\sigma$ ), and the number of states in which that pairing of methods converged.

these starting points are better at building in orbital relaxation effects than CIS or TD-DFT. There also appears to be a small advantage in terms of how easy it is to converge our CC equations, with EOM-CCSD and ESMF appearing to offer starting points closer to the ASCC or PLASCC solution points, or, at least, starting points from which the ASCC and PLASCC calculations are more likely to converge.

Overall, however, the main takeaway is not in the differences between results from different starting points, but in

how similar they are. PLASCC, for example, converts starting points from methods with MUEs of 0.87, 0.72, 0.36, and 0.11 eV in Figure 1 into results with MUEs of 0.12 eV or less. These uniformly small errors come despite the fact that the starting points contain very different amounts of post-excitation orbital relaxations: CIS and TD-DFT only relax the shape of the particle and hole orbital, EOM-CCSD also contains linearized relaxations for other orbitals, and ESMF offers full nonlinear relaxations for all orbitals. Nonetheless,

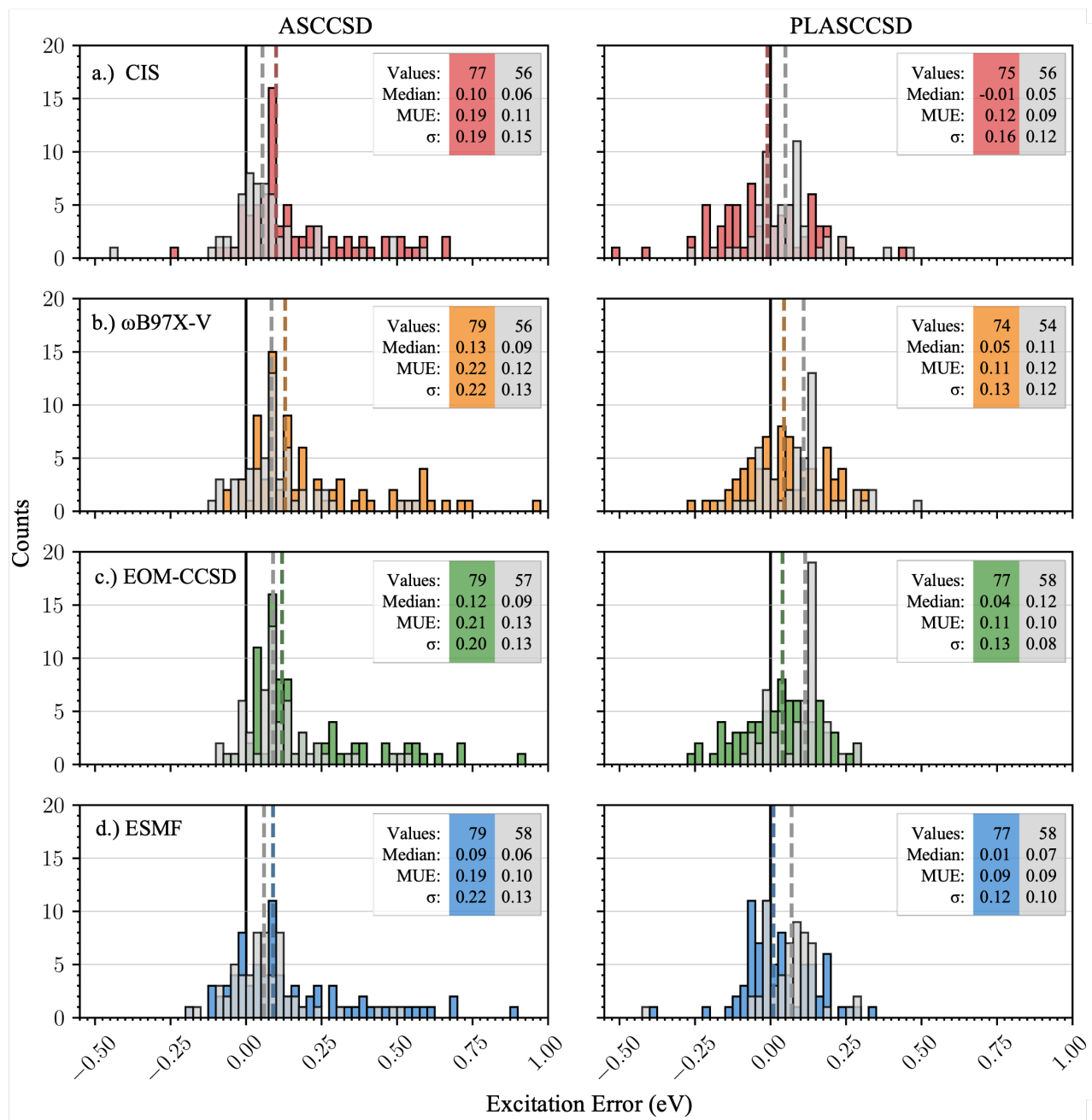


FIG. 3. ASCC (left) and PLASCC (right) excitation energy error distributions for different starting points broken out by state type: results for valence states are shown in color and those for Rydberg states in gray. Dashed lines show median errors, while these along with the MUEs, standard deviations, and number of converged states are shown in the insets.

Figure 2 shows that the ASCC and PLASCC error distributions are nearly independent of starting point, which appears to confirm that their exponentiated singles operators are indeed capable of building in orbital relaxations that may be missing in the starting point. We find it particularly noteworthy that when starting from CIS and TD-DFT, the simplest and most widely available starting points, PLASCC cleans things up to the point that typical errors are reduced to one or two tenths of an eV, and are nearly as good as when starting from

EOM-CCSD and ESMF.

In Figure 3, we break down these results into separate histograms for valence and Rydberg states. Even within each category, we see the same pattern: the results are quite insensitive to the choice of starting point. This breakout also reveals that PLASCC's accuracy advantage over ASCC appears to be concentrated in valence states, as the two approaches show much more comparable errors in Rydberg states. Again, PLASCC shows the best accuracy overall, and its accuracy is

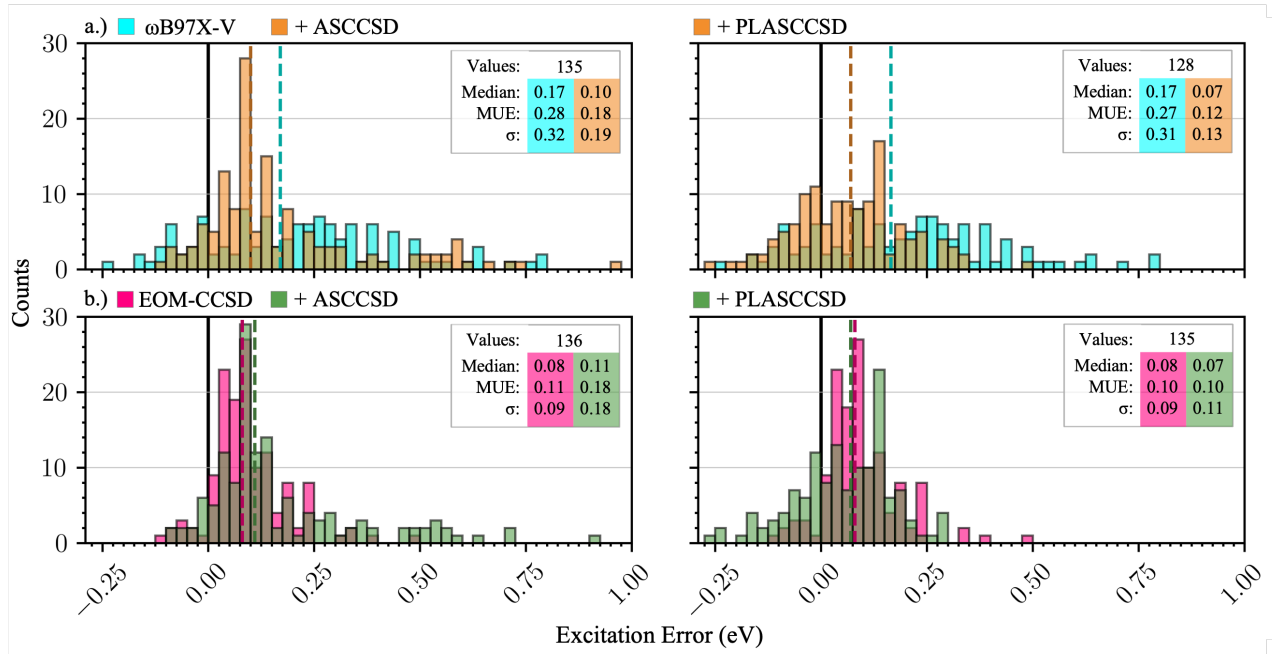


FIG. 4. Excitation energy error distributions on our reduced valence and Rydberg set for TD-DFT/ $\omega$ B97X-V (a) and EOM-CCSD (b) before and after post-linear-response treatments with ASCC and PLASCC. Dashed lines show median errors, with additional statistics in the insets.

slightly higher for the EOM-CCSD and ESMF starting points, but not by much. It is especially noteworthy to see that, in contrast to TD-DFT’s well known difficulties in Rydberg states,<sup>98</sup> PLASCC based on a TD-DFT starting point performs almost as well for these states as it does when based on ESMF.

Finally, in Figure 4, we show the combined valence and Rydberg error distributions for TD-DFT and EOM-CCSD before and after applying our ASCC or PLASCC post-linear-response treatment. While ASCC improves on the TD-DFT starting point, it goes in the wrong direction when starting from the already high-accuracy EOM-CCSD results. PLASCC, on the other hand, more or less maintains the high accuracy of EOM-CCSD while significantly improving on TD-DFT. At first glance, it therefore appears that there may not be much reason to favor PLASCC over EOM-CCSD for valence and Rydberg states. However, given the recent findings that nested PLASCC offers similarly high accuracies at greatly reduced cost,<sup>19</sup> it may in future be worthwhile to apply the nested theory as a low-cost, post-linear-response correction atop TD-DFT.

#### d. Charge transfer states

In Figure 5, we see that even in cases where the starting point method makes multi-eV errors in predicting a charge transfer energy, ASCC and especially PLASCC calculations based on that starting point tend to be quite accurate. Although the CIS starting point proved to be poor enough to prevent PLASCC from converging in two cases, post-linear-response PLASCC makes dramatic improvements in the other five CIS cases and in six of the seven TD-DFT cases. Overall,

when PLASCC is started from TD-DFT, it produces a MUE that is 20 times smaller than that of TD-DFT itself, which is especially remarkable given that the functional in question is a range-separated hybrid with dispersion corrections and thus is relatively well prepared for charge transfers between the molecules of a dimer. The improvement when starting from EOM-CCSD is less dramatic, but still significant, with the MUE lowered by a factor of more than three. As in the valence and Rydberg states, starting from ESMF provides a small advantage, but it is far from clear that reducing the MUE by 0.02 eV is worth forgoing the convenience of setting up the starting point via linear response theory.

## IV. CONCLUSION

We have found that Aufbau suppressed coupled cluster is quite insensitive to its starting point, which allows it to produce high-accuracy predictions when used in a post-linear-response mode with a range of linear response starting points. Even in cases where the underlying linear response theory is inaccurate — such as when modeling charge transfer states with time-dependent density functional theory — the post-linear-response coupled cluster treatment tends to produce accurate results. While starting from excited state mean field does appear to offer a (very) small accuracy boost, the fact that that method must perform a nonlinear orbital optimization one state at a time suggests that, for many practical applications, the more easily generated linear response starting points may be preferred.

Looking forward, there appear to be multiple ways to exploit the approach’s insensitivity to its starting point. Al-



though we have not tested it here, the CC2 method now seems quite promising as a starting point, given that its  $N^5$  cost scaling would go well with our recently-developed strategy of nesting a small excited state coupled cluster evaluation within its own non-iterative  $N^5$  second order perturbation theory. That said, CC2's cost is iterative  $N^5$ , and so one may also wonder whether the difficulties seen here for the even more affordable configuration interaction singles method could be addressed via modest, selective configuration interaction style expansions of its determinant basis. For that matter, transition density matrices and natural orbitals from selective configuration interaction itself may also be effective. There is likely also scope to improve the convergence chances of ASCC and PLASCC for all starting points by improving their amplitude equation Jacobians. We look forward to continuing to explore the opportunities created by Aufbau suppressed coupled cluster's starting point insensitivity in the future.

## ACKNOWLEDGMENTS

This work was supported by the National Science Foundation, Award Number 2320936. Computational work was performed with the LBNL Lawrence cluster and the Savio computational cluster resource provided by the Berkeley Research Computing program at the University of California, Berkeley. T.K.Q. and H.T. acknowledge that this material is based upon work supported by the National Science Foundation Graduate Research Fellowship Program under Grant No. DGE 2146752. Any opinions, findings, and conclusions or recommendations expressed in this material are those of the authors and do not necessarily reflect the views of the National Science Foundation.

## DATA AVAILABILITY STATEMENT

The data that support the findings of this study are available within the article and its supplementary material.

## REFERENCES

- <sup>1</sup>Shea, J. A. R.; Neuscamman, E. Communication: A mean field platform for excited state quantum chemistry. *The Journal of Chemical Physics* **2018**, *149*, 081101.
- <sup>2</sup>Shea, J. A. R.; Gwin, E.; Neuscamman, E. A Generalized Variational Principle with Applications to Excited State Mean Field Theory. *Journal of Chemical Theory and Computation* **2020**, *16*, 1526–1540, Publisher: American Chemical Society.
- <sup>3</sup>Hardikar, T. S.; Neuscamman, E. A self-consistent field formulation of excited state mean field theory. *The Journal of Chemical Physics* **2020**, *153*, 164108.
- <sup>4</sup>Hait, D.; Head-Gordon, M. Excited state orbital optimization via minimizing the square of the gradient: General approach and application to singly and doubly excited states via density functional theory. *Journal of chemical theory and computation* **2020**, *16*, 1699–1710.
- <sup>5</sup>Hait, D.; Head-Gordon, M. Highly accurate prediction of core spectra of molecules at density functional theory cost: Attaining sub-electronvolt error from a restricted open-shell Kohn–Sham approach. *The journal of physical chemistry letters* **2020**, *11*, 775–786.

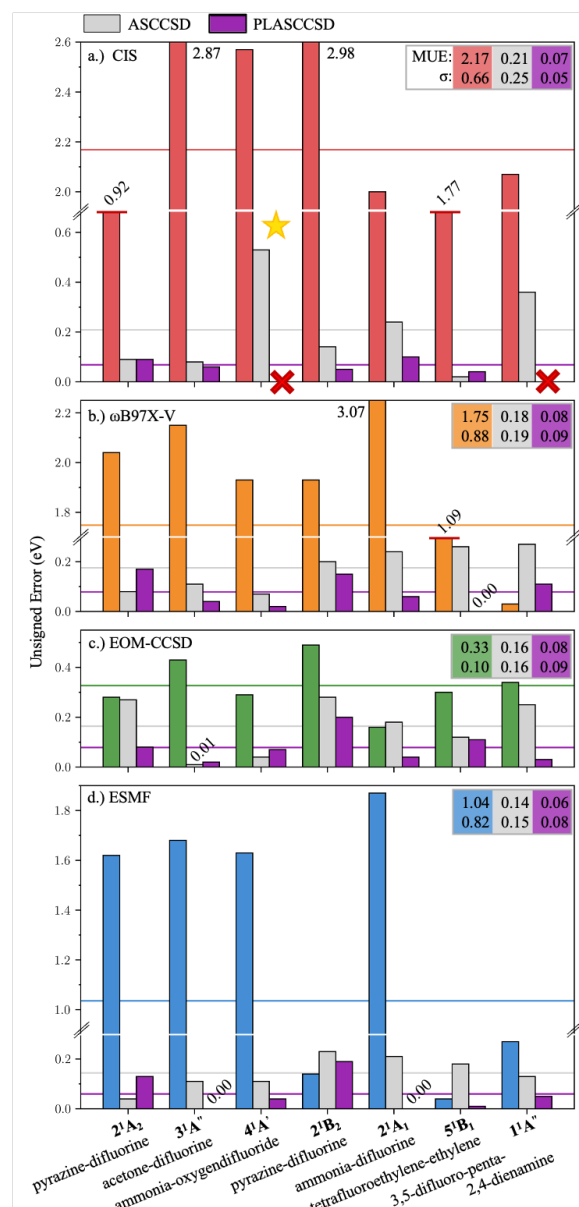


FIG. 5. Unsigned errors in charge transfer excitation energies. Errors for the starting point methods are shown in red (CIS), orange (TD-DFT/ $\omega$ B97X-V), green (EOM-CCSD), and blue (ESMF). Errors for ASCC and PLASCC based on these starting points are shown in gray and purple, respectively. Summarizing statistics across these seven states are provided in the insets, and horizontal lines depict the MUEs. Note the breaks in the vertical axes, and that we print the number for the unsigned error at the top of bars that do not fit on the plot. Red “x” marks indicate cases in which ASCC or PLASCC did not converge, and the yellow star indicates the one starting point that was two-CSF.

<sup>6</sup>Hait, D.; Head-Gordon, M. Orbital optimized density functional theory for electronic excited states. *The journal of physical chemistry letters* **2021**, *12*, 4517–4529.

<sup>7</sup>Tran, L. N.; Shea, J. A.; Neuscamman, E. Tracking excited states in wave function optimization using density matrices and variational principles.



- Journal of chemical theory and computation* **2019**, *15*, 4790–4803.
- <sup>8</sup> Tran, L. N.; Neuscamman, E. Improving excited-state potential energy surfaces via optimal orbital shapes. *The Journal of Physical Chemistry A* **2020**, *124*, 8273–8279.
  - <sup>9</sup> Tran, L. N.; Neuscamman, E. Exploring Ligand-to-Metal Charge-Transfer States in the Photo-Ferrioxalate System Using Excited-State Specific Optimization. *The Journal of Physical Chemistry Letters* **2023**, *14*, 7454–7460.
  - <sup>10</sup> Garner, S. M.; Haugen, E. A.; Leone, S. R.; Neuscamman, E. Spin coupling effect on geometry-dependent x-ray absorption of diradicals. *Journal of the American Chemical Society* **2024**, *146*, 2387–2397.
  - <sup>11</sup> Crawford, T. D.; Schaefer III, H. F. An introduction to coupled cluster theory for computational chemists. *Reviews in computational chemistry* **2007**, *14*, 33–136.
  - <sup>12</sup> Bartlett, R. J.; Musiał, M. Coupled-cluster theory in quantum chemistry. *Reviews of Modern Physics* **2007**, *79*, 291.
  - <sup>13</sup> Shavitt, I.; Bartlett, R. J. *Many-body methods in chemistry and physics: MBPT and coupled-cluster theory*; Cambridge university press, 2009.
  - <sup>14</sup> Hampel, C.; Peterson, K. A.; Werner, H.-J. A comparison of the efficiency and accuracy of the quadratic configuration interaction (QCISD), coupled cluster (CCSD), and Brueckner coupled cluster (BCCD) methods. *Chemical physics letters* **1992**, *190*, 1–12.
  - <sup>15</sup> Lee, T. J.; Kobayashi, R.; Handy, N. C.; Amos, R. D. Comparison of the Brueckner and coupled-cluster approaches to electron correlation. *The Journal of chemical physics* **1992**, *96*, 8931–8937.
  - <sup>16</sup> Bertels, L. W.; Lee, J.; Head-Gordon, M. Polishing the gold standard: The role of orbital choice in CCSD (T) vibrational frequency prediction. *Journal of chemical theory and computation* **2021**, *17*, 742–755.
  - <sup>17</sup> Tuckman, H.; Neuscamman, E. Aufbau Suppressed Coupled Cluster Theory for Electronically Excited States. *Journal of Chemical Theory and Computation* **2024**, *20*, 2761–2773, Publisher: American Chemical Society.
  - <sup>18</sup> Tuckman, H.; Ma, Z.; Neuscamman, E. Improving Aufbau Suppressed Coupled Cluster through Perturbative Analysis. *Journal of Chemical Theory and Computation* **2025**, Publisher: American Chemical Society.
  - <sup>19</sup> Tuckman, H.; Neuscamman, E. Fast and Accurate Charge Transfer Excitations via Nested Aufbau Suppressed Coupled Cluster. *arXiv.org* **2025**, 2505.17299.
  - <sup>20</sup> Thouless, D. J. Stability conditions and nuclear rotations in the Hartree-Fock theory. *Nuclear Physics* **1960**, *21*, 225–232.
  - <sup>21</sup> Dreuw, A.; Head-Gordon, M. Single-reference ab initio methods for the calculation of excited states of large molecules. *Chemical reviews* **2005**, *105*, 4009–4037.
  - <sup>22</sup> Runge, E.; Gross, E. K. Density-functional theory for time-dependent systems. *Physical review letters* **1984**, *52*, 997.
  - <sup>23</sup> Burke, K.; Werschnik, J.; Gross, E. Time-dependent density functional theory: Past, present, and future. *The Journal of chemical physics* **2005**, *123*, 062206.
  - <sup>24</sup> Casida, M. E.; Huix-Rotllant, M. Progress in time-dependent density-functional theory. *Annual review of physical chemistry* **2012**, *63*, 287–323.
  - <sup>25</sup> Rowe, D. Equations-of-motion method and the extended shell model. *Reviews of Modern Physics* **1968**, *40*, 153.
  - <sup>26</sup> Stanton, J. F.; Bartlett, R. J. The equation of motion coupled-cluster method. A systematic biorthogonal approach to molecular excitation energies, transition probabilities, and excited state properties. *The Journal of chemical physics* **1993**, *98*, 7029–7039.
  - <sup>27</sup> Krylov, A. I. Equation-of-motion coupled-cluster methods for open-shell and electronically excited species: The hitchhiker's guide to Fock space. *Annu. Rev. Phys. Chem.* **2008**, *59*, 433–462.
  - <sup>28</sup> Monkhorst, H. J. Calculation of properties with the coupled-cluster method. *International Journal of Quantum Chemistry* **1977**, *12*, 421–432.
  - <sup>29</sup> Dalgaard, E.; Monkhorst, H. J. Some aspects of the time-dependent coupled-cluster approach to dynamic response functions. *Physical Review A* **1983**, *28*, 1217.
  - <sup>30</sup> Sekino, H.; Bartlett, R. J. A linear response, coupled-cluster theory for excitation energy. *International Journal of Quantum Chemistry* **1984**, *26*, 255–265.
  - <sup>31</sup> Koch, H.; Jørgensen, P. Coupled cluster response functions. *The Journal of chemical physics* **1990**, *93*, 3333.
  - <sup>32</sup> Rico, R. J.; Head-Gordon, M. Single-reference theories of molecular excited states with single and double substitutions. *Chemical physics letters* **1993**, *213*, 224–232.
  - <sup>33</sup> Koch, H.; Kobayashi, R.; Sanchez de Merás, A.; Jørgensen, P. Calculation of size-intensive transition moments from the coupled cluster singles and doubles linear response function. *The Journal of chemical physics* **1994**, *100*, 4393–4400.
  - <sup>34</sup> Sneskov, K.; Christiansen, O. Excited state coupled cluster methods. *Wiley Interdisciplinary Reviews: Computational Molecular Science* **2012**, *2*, 566–584.
  - <sup>35</sup> Subotnik, J. E. Communication: Configuration interaction singles has a large systematic bias against charge-transfer states. *The Journal of chemical physics* **2011**, *135*, 071104.
  - <sup>36</sup> Herbert, J. M. *Theoretical and computational photochemistry*; Elsevier, 2023; pp 69–118.
  - <sup>37</sup> Sobolewski, A. L.; Domcke, W. Ab initio study of the excited-state coupled electron–proton-transfer process in the 2-aminopyridine dimer. *Chemical Physics* **2003**, *294*, 73–83.
  - <sup>38</sup> Dreuw, A.; Weisman, J. L.; Head-Gordon, M. Long-range charge-transfer excited states in time-dependent density functional theory require non-local exchange. *The Journal of chemical physics* **2003**, *119*, 2943–2946.
  - <sup>39</sup> Dreuw, A.; Head-Gordon, M. Failure of time-dependent density functional theory for long-range charge-transfer excited states: the zincbacteriochlorin- bacteriochlorin and bacteriochlorophyll- spheroidene complexes. *Journal of the American Chemical Society* **2004**, *126*, 4007–4016.
  - <sup>40</sup> Mester, D.; Kállay, M. Charge-transfer excitations within density functional theory: how accurate are the most recommended approaches? *Journal of Chemical Theory and Computation* **2022**, *18*, 1646–1662.
  - <sup>41</sup> Kozma, B.; Tajti, A.; Demoulin, B.; Izsák, R.; Nooijen, M.; Szalay, P. G. A new benchmark set for excitation energy of charge transfer states: systematic investigation of coupled cluster type methods. *Journal of Chemical Theory and Computation* **2020**, *16*, 4213–4225.
  - <sup>42</sup> Izsák, R. Single-reference coupled cluster methods for computing excitation energies in large molecules: The efficiency and accuracy of approximations. *Wiley Interdisciplinary Reviews: Computational Molecular Science* **2020**, *10*, e1445.
  - <sup>43</sup> Coriani, S.; Christiansen, O.; Fransson, T.; Norman, P. Coupled-cluster response theory for near-edge x-ray-absorption fine structure of atoms and molecules. *Physical Review A—Atomic, Molecular, and Optical Physics* **2012**, *85*, 022507.
  - <sup>44</sup> Frati, F.; De Groot, F.; Cerezo, J.; Santoro, F.; Cheng, L.; Faber, R.; Coriani, S. Coupled cluster study of the x-ray absorption spectra of formaldehyde derivatives at the oxygen, carbon, and fluorine K-edges. *The Journal of Chemical Physics* **2019**, *151*, 064107.
  - <sup>45</sup> Domingo, A.; Carvajal, M. À.; de Graaf, C.; Sivalingam, K.; Neese, F.; Angeli, C. Metal-to-metal charge-transfer transitions: reliable excitation energies from ab initio calculations. *Theor. Chem. Acc.* **2012**, *131*, 1264.
  - <sup>46</sup> Pineda Flores, S. D.; Neuscamman, E. Excited state specific multi-Slater Jastrow wave functions. *The Journal of Physical Chemistry A* **2019**, *123*, 1487–1497.
  - <sup>47</sup> Clune, R.; Neuscamman, E. An excitation matched local correlation approach to excited state specific perturbation theory. *arXiv* **2025**, 2505.08659.
  - <sup>48</sup> Ye, H.-Z.; Welborn, M.; Rieke, N. D.; Van Voorhis, T.  $\sigma$ -SCF: A direct energy-targeting method to mean-field excited states. *The Journal of chemical physics* **2017**, *147*, 214104.
  - <sup>49</sup> Ye, H.-Z.; Van Voorhis, T. Half-projected  $\sigma$  self-consistent field for electronic excited states. *Journal of chemical theory and computation* **2019**, *15*, 2954–2965.
  - <sup>50</sup> Bagus, P. S. Self-consistent-field wave functions for hole states of some Ne-like and Ar-like ions. *Phys. Rev.* **1965**, *139*, A619.
  - <sup>51</sup> Hsu, H.-I.; Davidson, E. R.; Pitzer, R. M. An SCF method for hole states. *J. Chem. Phys.* **1976**, *65*, 609–613.
  - <sup>52</sup> Naves de Brito, A.; Correia, N.; Svensson, S.; Ågren, H. A theoretical study of x-ray photoelectron spectra of model molecules for polymethyl-methacrylate. *J. Chem. Phys.* **1991**, *95*, 2965–2974.
  - <sup>53</sup> Besley, N. A.; Gilbert, A. T.; Gill, P. M. Self-consistent-field calculations of core excited states. *The Journal of chemical physics* **2009**, *130*, 124308.
  - <sup>54</sup> Filatov, M.; Shaik, S. A spin-restricted ensemble-referenced Kohn-Sham method and its application to diradicaloid situations. *Chem. Phys. Lett.* **1999**, *304*, 429–437.

- <sup>55</sup>Kowalczyk, T.; Tsuchimochi, T.; Chen, P.-T.; Top, L.; Van Voorhis, T. Excitation energies and Stokes shifts from a restricted open-shell Kohn-Sham approach. *The Journal of chemical physics* **2013**, *138*, 164101.
- <sup>56</sup>Kowalczyk, T.; Yost, S. R.; Voorhis, T. V. Assessment of the  $\Delta$ SCF density functional theory approach for electronic excitations in organic dyes. *The Journal of chemical physics* **2011**, *134*.
- <sup>57</sup>Zhao, L.; Neuscamman, E. Density functional extension to excited-state mean-field theory. *Journal of chemical theory and computation* **2019**, *16*, 164–178.
- <sup>58</sup>Levi, G.; Ivanov, A. V.; Jónsson, H. Variational density functional calculations of excited states via direct optimization. *Journal of Chemical Theory and Computation* **2020**, *16*, 6968–6982.
- <sup>59</sup>Kempfer-Robertson, E. M.; Haase, M. N.; Bersson, J. S.; Avdic, I.; Thompson, L. M. Role of Exact Exchange in Difference Projected Double-Hybrid Density Functional Theory for Treatment of Local, Charge Transfer, and Rydberg Excitations. *The Journal of Physical Chemistry A* **2022**, *126*, 8058–8069.
- <sup>60</sup>Gilbert, A. T.; Besley, N. A.; Gill, P. M. Self-consistent field calculations of excited states using the maximum overlap method (MOM). *The Journal of Physical Chemistry A* **2008**, *112*, 13164–13171.
- <sup>61</sup>Barca, G. M.; Gilbert, A. T.; Gill, P. M. Simple models for difficult electronic excitations. *Journal of chemical theory and computation* **2018**, *14*, 1501–1509.
- <sup>62</sup>Carter-Fenk, K.; Herbert, J. M. State-targeted energy projection: A simple and robust approach to orbital relaxation of non-Aufbau self-consistent field solutions. *Journal of Chemical Theory and Computation* **2020**, *16*, 5067–5082.
- <sup>63</sup>Zhao, L.; Neuscamman, E. An efficient variational principle for the direct optimization of excited states. *Journal of chemical theory and computation* **2016**, *12*, 3436–3440.
- <sup>64</sup>Robinson, P. J.; Pineda Flores, S. D.; Neuscamman, E. Excitation variance matching with limited configuration interaction expansions in variational Monte Carlo. *The Journal of Chemical Physics* **2017**, *147*, 164114.
- <sup>65</sup>Blunt, N. S.; Neuscamman, E. Charge-transfer excited states: Seeking a balanced and efficient wave function ansatz in variational Monte Carlo. *The Journal of Chemical Physics* **2017**, *147*, 194101.
- <sup>66</sup>Shea, J. A.; Neuscamman, E. Size consistent excited states via algorithmic transformations between variational principles. *Journal of Chemical Theory and Computation* **2017**, *13*, 6078–6088.
- <sup>67</sup>Garner, S. M.; Neuscamman, E. A variational Monte Carlo approach for core excitations. *The Journal of chemical physics* **2020**, *153*, 144108.
- <sup>68</sup>Otis, L.; Craig, I. M.; Neuscamman, E. A hybrid approach to excited-state-specific variational Monte Carlo and doubly excited states. *The Journal of Chemical Physics* **2020**, *153*, 234105.
- <sup>69</sup>Shepard, S.; Panadés-Barrueta, R. L.; Moroni, S.; Scemama, A.; Filippi, C. Double excitation energies from quantum Monte Carlo using state-specific energy optimization. *Journal of chemical theory and computation* **2022**, *18*, 6722–6731.
- <sup>70</sup>Otis, L.; Neuscamman, E. Optimization stability in excited-state-specific Variational Monte Carlo. *Journal of Chemical Theory and Computation* **2023**, *19*, 767–782.
- <sup>71</sup>Otis, L.; Neuscamman, E. A promising intersection of excited-state-specific methods from quantum chemistry and quantum Monte Carlo. *Wiley Interdisciplinary Reviews: Computational Molecular Science* **2023**, *13*, e1659.
- <sup>72</sup>Pathak, S.; Busemeyer, B.; Rodrigues, J. N.; Wagner, L. K. Excited states in variational Monte Carlo using a penalty method. *The Journal of Chemical Physics* **2021**, *154*, 034101.
- <sup>73</sup>Entwistle, M. T.; Schätzle, Z.; Erdman, P. A.; Hermann, J.; Noé, F. Electronic excited states in deep variational Monte Carlo. *Nature Communications* **2023**, *14*, 274.
- <sup>74</sup>Hanscam, R.; Neuscamman, E. Applying generalized variational principles to excited-state-specific complete active space self-consistent field theory. *Journal of Chemical Theory and Computation* **2022**, *18*, 6608–6621.
- <sup>75</sup>Roos, B. O.; Andersson, K.; Fülcher, M. P. Towards an accurate molecular orbital theory for excited states: the benzene molecule. *Chemical Physics Letters* **1992**, *192*, 5–13.
- <sup>76</sup>Boyn, J.-N.; Mazziotti, D. A. Elucidating the molecular orbital dependence of the total electronic energy in multireference problems. *The Journal of Chemical Physics* **2022**, *156*, 194104.
- <sup>77</sup>Clune, R.; Shea, J. A.; Neuscamman, E. N5-scaling excited-state-specific perturbation theory. *Journal of chemical theory and computation* **2020**, *16*, 6132–6141.
- <sup>78</sup>Clune, R.; Shea, J. A.; Hardikar, T. S.; Tuckman, H.; Neuscamman, E. Studying excited-state-specific perturbation theory on the Thiel set. *The Journal of Chemical Physics* **2023**, *158*.
- <sup>79</sup>Mayhall, N. J.; Raghavachari, K. Multiple solutions to the single-reference CCSD equations for NiH. *Journal of Chemical Theory and Computation* **2010**, *6*, 2714–2720.
- <sup>80</sup>Zheng, X.; Cheng, L. Performance of delta-coupled-cluster methods for calculations of core-ionization energies of first-row elements. *Journal of chemical theory and computation* **2019**, *15*, 4945–4955.
- <sup>81</sup>Lee, J.; Small, D. W.; Head-Gordon, M. Excited states via coupled cluster theory without equation-of-motion methods: Seeking higher roots with application to doubly excited states and double core hole states. *The Journal of chemical physics* **2019**, *151*, 214103.
- <sup>82</sup>Damour, Y.; Scemama, A.; Jacquemin, D.; Kossoski, F.; Loos, P.-F. State-specific coupled-cluster methods for excited states. *Journal of Chemical Theory and Computation* **2024**.
- <sup>83</sup>Kossoski, F.; Marie, A.; Scemama, A.; Caffarel, M.; Loos, P.-F. Excited States from State-Specific Orbital-Optimized Pair Coupled Cluster. *Journal of Chemical Theory and Computation* **2021**, *17*, 4756–4768.
- <sup>84</sup>Tuckman, H.; Neuscamman, E. Excited-State-Specific Pseudoprojected Coupled-Cluster Theory. *Journal of Chemical Theory and Computation* **2023**, *19*, 6160–6171, Publisher: American Chemical Society.
- <sup>85</sup>Liu, X.; Fatehi, S.; Shao, Y.; Veldkamp, B. S.; Subotnik, J. E. Communication: Adjusting charge transfer state energies for configuration interaction singles: Without any parameterization and with minimal cost. *The Journal of chemical physics* **2012**, *136*, 161101.
- <sup>86</sup>Kossoski, F.; Loos, P.-F. State-specific configuration interaction for excited states. *Journal of Chemical Theory and Computation* **2023**, *19*, 2258–2269.
- <sup>87</sup>Kossoski, F.; Loos, P.-F. Seniority and hierarchy configuration interaction for radicals and excited states. *Journal of Chemical Theory and Computation* **2023**, *19*, 8654–8670.
- <sup>88</sup>Burton, H. G. Energy Landscape of State-Specific Electronic Structure Theory. *Journal of Chemical Theory and Computation* **2022**, *18*, 1512–1526.
- <sup>89</sup>Tsuchimochi, T. Double configuration interaction singles: Scalable and size-intensive approach for orbital relaxation in excited states and bond-dissociation. *The Journal of Chemical Physics* **2024**, *161*.
- <sup>90</sup>Loos, P.-F.; Scemama, A.; Blondel, A.; Garniron, Y.; Caffarel, M.; Jacquemin, D. A Mountaineering Strategy to Excited States: Highly Accurate Reference Energies and Benchmarks. *Journal of Chemical Theory and Computation* **2018**, *14*, 4360–4379, Publisher: American Chemical Society.
- <sup>91</sup>Loos, P.-F.; Lipparini, F.; Boggio-Pasqua, M.; Scemama, A.; Jacquemin, D. A Mountaineering Strategy to Excited States: Highly Accurate Energies and Benchmarks for Medium Sized Molecules. *Journal of Chemical Theory and Computation* **2020**, *16*, 1711–1741, Publisher: American Chemical Society.
- <sup>92</sup>Martin, R. L. Natural transition orbitals. *The Journal of chemical physics* **2003**, *118*, 4775–4777.
- <sup>93</sup>Eckart, C.; Young, G. The approximation of one matrix by another of lower rank. *Psychometrika* **1936**, *1*, 211–218.
- <sup>94</sup>Furche, F. On the density matrix based approach to time-dependent density functional response theory. *The Journal of Chemical Physics* **2001**, *114*, 5982–5992.
- <sup>95</sup>Sun, Q.; Zhang, X.; Banerjee, S.; Bao, P.; Barbry, M.; Blunt, N. S.; Bogdanov, N. A.; Booth, G. H.; Chen, J.; Cui, Z.-H.; others Recent developments in the PySCF program package. *The Journal of chemical physics* **2020**, *153*, 024109.
- <sup>96</sup>Mardirossian, N.; Head-Gordon, M.  $\omega$ B97X-V: A 10-parameter, range-separated hybrid, generalized gradient approximation density functional with nonlocal correlation, designed by a survival-of-the-fittest strategy. *Physical Chemistry Chemical Physics* **2014**, *16*, 9904–9924.
- <sup>97</sup>Epifanovsky, E.; Gilbert, A. T.; Feng, X.; Lee, J.; Mao, Y.; Mardirossian, N.; Pokhilko, P.; White, A. F.; Coons, M. P.; Dempwolff, A. L.; others Software for the frontiers of quantum chemistry: An overview of developments in the Q-Chem 5 package. *The Journal of chemical physics* **2021**, *155*.

<sup>98</sup>Laurent, A. D.; Jacquemin, D. TD-DFT benchmarks: a review. *International Journal of Quantum Chemistry* **2013**, *113*, 2019–2039.

## V. SUPPLEMENTARY INFORMATION

### a. Multi-CSF and State Inclusion Details

The determination of the wave function being single or multi-CSF is starting point dependent. Of the 138 valence and Rydberg states 14 were considered two-CSF by ESMF, 23 by CIS, 22 by  $\omega$ B97X-V, and 23 by EOM-CCSD. In Fig. S1 we breakdown the results of ASCC and PLASCC on the QUEST set of valence and Rydberg states by one-CSF, shown in color, or two-CSF shown in yellow. This delineation between the different CSF type wave functions reveals that the two-CSF states consistently overestimate the excitation energies relative to the one-CSF states. When compared to ASCC, PLASCC slightly improves on

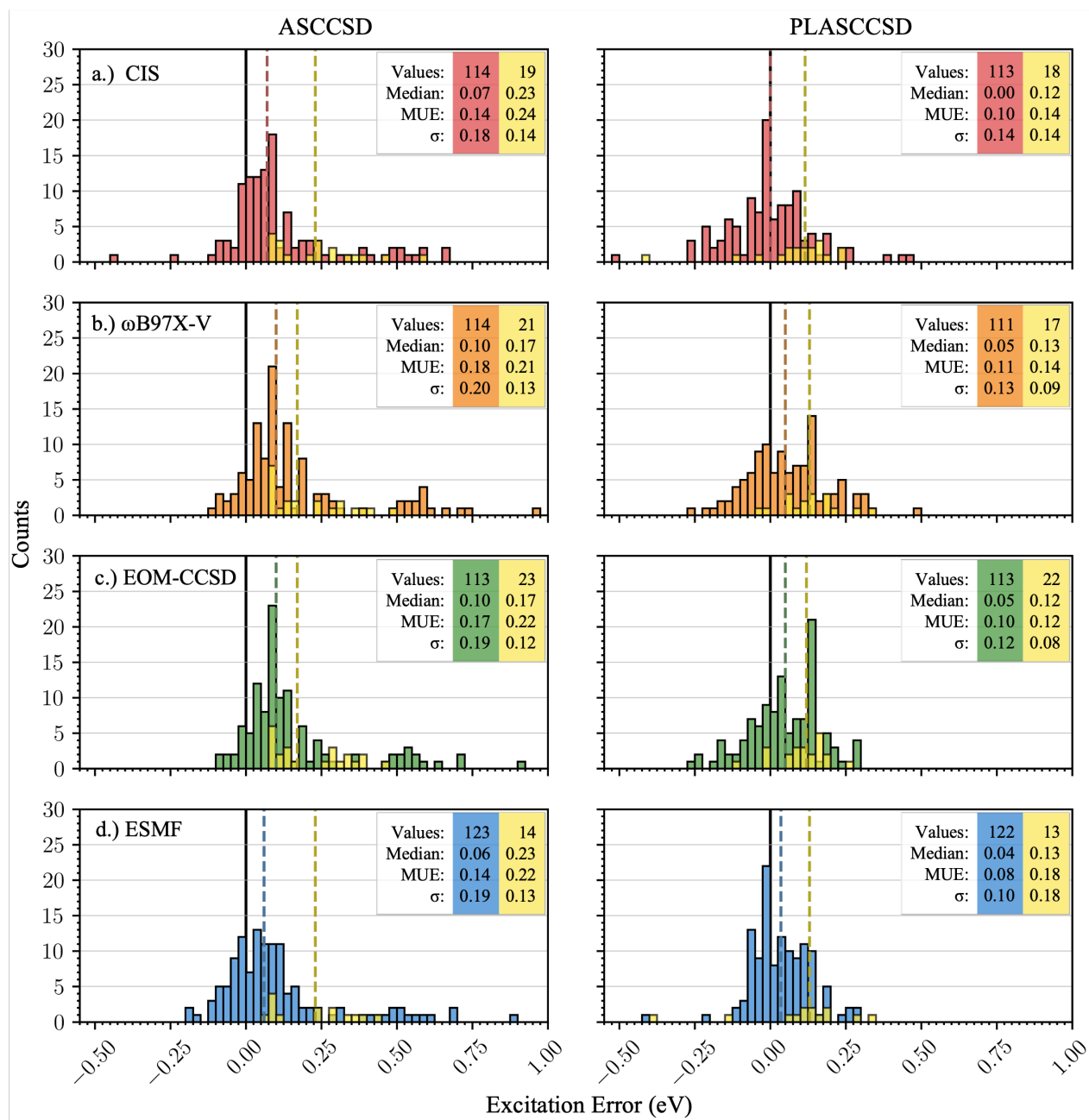


FIG. S1. ASCC (left) and PLASCC (right) excitation energy error distributions on the QUEST valence and Rydberg states for different starting points broken out by one-CSF (shown in color) or two-CSF (shown in yellow). Dashed lines show median errors, while these along with the MUEs, standard deviations, and number of converged states are shown in the insets.

the two-CSF states, reducing the median relative to ASCC anywhere from 0.04 to 0.11 eV. Moving on to the specifics of the winnowing procedure among our reduced valence and Rydberg test set, five individual cases were removed for being two-CSF with more than four non-hydrogen atoms. These include four CIS states — thiophene  $1^1B_1$ , tetrazine  $1^1B_{2g}$ , pyrazine  $2^1B_{1g}$ , and pyrimidine  $2^1B_1$  — and one  $\omega$ B97X-V state — thiophene  $2^1B_2$ . The  $\omega$ B97X-V reference for pyridazine  $1^1B_2$  was omitted due to being a three-CSF. Six states across ASCCSD and PLASCCSD were not reported due to convergence issues, specifically ammonia  $2^1A_2$  using an EOM-CCSD reference for ASCC and five  $\omega$ B97X-V states — formaldehyde  $1^1B_2$ , formamide  $3^1A'$ , isobutene  $1^1B_1$ , thioacetone  $2^1A_1$ , and cyclopropenone  $3^1B_2$  — for PLASCC. Lastly in the Quest set of result, all four references were removed for furan  $2^1B_2$  in ASCC and cyclopropenethione  $1^1B_2$  and  $1^1B_2$  as well as diacetylene  $1^1\Delta_u$  in PLASCC due to not having results in at least two of the references considered. In the charge transfer set, PLASCC results on two CIS states — ammonia-oxygendifluoride  $4^1A'$  and 3,5-difluoro-penta-2,4-dienamine  $1^1A''$  — are left unreported due to convergence issues.

## b. Raw Data

The table below includes excitation energies (eV) of EMSF, CIS, TD-DFT/ $\omega$ B97X-V, and EOM-CCSD along with their corresponding ASCCSD and PLASCCSD counterparts. The 'Flip' column indicates states with two similar but distinct ansatz choices for the ASCC framework.<sup>18</sup> Both energies are reported. The 'Rydberg' column indicates Rydberg states plotted separately in Fig. 3, as designated by the QUEST small and medium sets. The ' $n$ -CSF' column indicates how many singular values were  $>0.2$  when forming the reference for each of the four methods (only  $n=1$  or  $2$  were calculated). The 'REF' column are reference energies. Reference energies for the QUEST small and medium sets are at exFCI for molecules with three or fewer non-hydrogen atoms and EOM-CCSDT otherwise unless explicitly stated. Reference energies for the charge transfer set are at EOM-CCSDT unless explicitly stated.

Table annotations: \*States are loosely converged, but energetically change below precision reported iteration by iteration. (a) EOM-CCSDTQ reference. (b) EOM-CCSDT reference. (c) LR-CC3 reference.

Molecule	State	Flip	Rydberg	REF	Excitation energy (eV)			ASCC excitation energy (eV)			PLASCC excitation energy (eV)		
					<i>n</i> -CSF			<i>w</i> B97X-V			<i>CIS</i>		
					ESMF	<i>CIS</i>	<i>EOM-CCSD</i>	ESMF	<i>CIS</i>	<i>w</i> B97X-V	ESMF	<i>CIS</i>	<i>w</i> B97X-V
H2O	11B1		R	7.53	1	1	1	7.50	7.54	7.54	7.51	7.52	7.50
H2O	11A2		R	9.32	1	1	1	9.27	9.33	9.32	9.28	9.29	9.28
H2O	21A1	Y		9.94	1	1	1	9.86	9.94	9.87	9.90	9.97	9.86
H2S	11B1		R	6.10	1	1	1	6.12	6.12	6.13	6.11	6.10	6.11
H2S	11A2		R	6.29	1	1	1	6.28	6.28	6.29	6.28	6.27	6.27
Ammonia	11A2	Y		6.48	1	1	1	6.42	6.47	6.44	6.46	6.41	6.46
Ammonia	11E		R	8.08	1	1	1	8.03	8.05	8.05	8.06	8.04	8.03
Ammonia	21A1	Y		9.68	1	1	1	9.65	9.62	9.41	9.64	9.57	9.49
Ammonia	21A2	Y		10.41	1	1	1	10.45	10.31	10.41	10.40	10.38	10.38
HCl	1pi			7.82	1	1	1	7.82	7.84	7.84	7.82	7.82	7.81
N2	11pi <sub>g</sub>			9.41	1	1	1	9.64	9.63	9.65	9.46	9.44	9.45
N2	11sigu-			10.05	2	2	2	10.14	10.14	10.14	10.23	10.23	10.23
N2	11deltau			10.43	2	2	2	10.55	10.55	10.56	10.55	10.55	10.56
CO	11pi			8.57	1	1	1	8.66	8.67	8.70	8.59	8.50	8.54
CO	11sig-			10.05	2	2	2	10.12	10.12	10.14	10.17	10.16	10.17
CO	11del			10.16	2	2	2	10.26	10.26	10.29	10.26	10.22	10.24
CO	21sig+	Y		10.94	1	1	1	11.19	10.78	10.81	10.88	11.45	10.85
CO	31sig+	Y		11.52	1	1	1	11.48	11.21	10.97	11.51	11.29	11.67
CO	21pi		R	11.76	1	1	1	11.87	11.79	11.85	11.89	11.77	11.85
Acetylene	11sigu-			7.20	2	2	2	7.28	7.29	7.29	7.34	7.34	7.35
Acetylene	11delu			7.51	2	2	2	7.59	7.60	7.60	7.64	7.61	7.63
Ethylene	11B3u		R	7.31	1	1	1	7.22	7.22	7.23	7.31	7.29	7.30
Ethylene	11B1u			7.93	1	1	1	7.88	7.87	7.88	7.88	7.88	7.89
Ethylene	11B1g			8.00	1	1	1	7.91	7.91	7.92	8.00	7.98	8.00
Formaldehyde	11A2			3.99	1	1	1	3.95	4.05	4.07	3.95	3.94	3.94
Formaldehyde	11B2		R	7.11	1	1	1	7.11	7.21	7.21	7.09	7.16	7.10
Formaldehyde	21B2			8.04	1	1	1	8.08	8.18	8.19	8.05	8.06	8.08
Formaldehyde	21A2		R	8.65	1	1	1	8.72	8.78	8.78	8.69	8.69	8.72
Formaldehyde	11B1			9.29	1	1	1	9.27	9.37	9.39	9.27	9.30	9.32
Thioformaldehyde	11A2		(a)2.26		1	1	1	2.16	2.25	2.26	2.23	2.13	2.14
Thioformaldehyde	11B2			5.83	1	1	1	5.85	5.89	5.90	5.83	5.77	5.81
Thioformaldehyde	21A1	Y		6.51	1	1	2	6.61	6.64	6.62	6.74	6.50	6.62
Methanimine	11Ad			5.25	1	1	1	5.22	5.32	5.33	5.23	5.16	5.18
Acetaldehyde	11Ad			4.34	1	1	1	4.30	4.40	4.43	4.28	4.27	4.28
Cyclopropane	11B1		(b)6.71		1	2	1	6.77	6.82	6.82	6.74	6.74	6.71
Cyclopropane	11B2			6.82	1	1	1	6.86	6.86	6.88	6.78	6.78	6.80
Diazomethane	11A2			3.09	1	1	1	2.97	3.06	3.04	3.06	2.82	2.88
Diazomethane	11B1			5.35	1	1	1	5.31	5.29	5.32	5.34	5.33	5.37
Diazomethane	21A1	Y		5.79	1	1	2	5.84	5.80	5.93	5.81	5.75	5.88
Formamide	11A*			5.70	1	1	1	5.62	5.73	5.75	5.60	5.55	5.58
Formamide	21A*	Y		6.67	1	2	2	6.73	7.00	6.83	6.78	6.76	6.84
Formamide	31A*	Y		7.64	2	1	2	7.84	7.90	7.44	7.70	7.31	7.45
Formamide	41A*	Y		7.29	1	2	2	7.40	7.86	7.87	7.37	7.36	7.28
Ketene	11A2			3.84	1	1	1	3.84	3.88	3.91	3.82	3.74	3.79

Small QUEST set

Molecule	State	Flip	Rydberg	REF	n-CSF			Excitation energy (eV)			ASCC excitation energy (eV)			PLASCC excitation energy (eV)		
					ESMF	CIS	WB97X-V	ESMF	CIS	WB97X-V	ESMF	CIS	WB97X-V	ESMF	CIS	WB97X-V
Ketene	11B1	R	5.88		1	1	1	5.55	6.42	6.06	5.94	5.93	5.90	5.90	5.96	5.97
Ketene	21A2	R	7.08		1	1	1	6.52	7.53	7.20	7.15	7.10	7.08	7.08	7.13	7.15
Nitrosomethane	11A*		1.99		1	1	1	2.35	2.08	1.91	2.00	2.04	2.09	2.09	2.11	2.10
Streptocyanine-C1	11B2		7.14		1	1	1	7.26	8.55	7.94	7.22	7.19	7.19	7.22	7.25	7.25
acetone	11A2		4.48		1	1	1	3.67	5.23	4.54	4.53	4.47	4.58	4.58	4.61	4.60
acetone	11B2	R	6.30		1	1	1	5.76	8.26	6.73	6.40	6.47	6.56	6.56	6.57	6.55
acetone	21A1	Y	7.36		1	2	1	6.80	9.24	7.80	7.46	7.52	7.49	7.53	7.62	7.58
acetone	21A2	R	7.38		1	1	1	6.61	9.21	7.78	7.43	7.49	7.49	7.58	7.58	7.57
acetone	21B2	R	7.55		1	1	1	6.80	9.34	7.88	7.60	7.67	7.80	7.80	7.81	7.75
isobutene	11B1		6.39		1	1	1	5.43	6.63	6.52	6.44	6.41	6.41	6.41	6.43	6.43
isobutene	21A1	Y	7.00		1	1	1	6.14	7.13	7.10	7.06	7.07	6.99	7.01	7.02	7.04
thioacetone	11A2		2.57		1	1	1	1.92	3.23	2.68	2.65	2.48	2.57	2.57	2.60	2.61
thioacetone	11B2		5.43		1	1	1	5.00	6.37	5.93	5.82	5.52	5.52	5.57	5.59	5.56
thioacetone	21A1	Y	5.98		1	1	2	6.22	6.20	6.20	6.07	5.94	6.11	5.93	6.03	6.14
thioacetone	21B2		6.44		1	1	1	5.88	7.07	6.74	6.50	6.55	6.66	6.66	6.64	6.54
thioacetone	31A1	Y	6.53		1	1	1	5.74	7.37	7.04	6.61	6.51	6.50	6.49	6.52	6.62
cyanoformaldehyde	11A*		3.84		1	1	1	2.89	4.53	3.89	3.94	3.82	3.94	3.94	3.99	3.97
cyanoformaldehyde	21A*		6.54		1	1	1	5.36	6.14	5.97	6.77	6.56	6.63	6.63	6.60	6.61
propenal	11A*		3.82		1	1	1	2.94	4.63	3.92	3.93	3.80	3.92	3.92	3.95	3.95
propenal	21A*		5.62		1	1	1	4.69	5.30	5.05	5.77	5.43	5.62	5.62	5.65	5.67
thiopropenal	11A*		2.06		1	1	1	1.39	2.59	2.15	2.17	1.96	2.06	2.06	2.09	2.10
cyclopropenone	11B1		4.23		1	1	1	4.14	5.87	4.58	4.47	4.40	4.54	4.54	4.51	4.50
cyclopropenone	11A2		5.56		1	1	1	5.29	6.43	5.61	5.62	5.65	5.72	5.72	5.75	5.73
cyclopropenone	11B2	R	6.19		1	2	1	5.68	7.76	6.54	6.27	6.37	6.42	---	6.47	6.44
cyclopropenone	31B2	R	6.86		1	1	2	6.40	8.42	7.30	6.96	7.02	6.97	6.97	7.09	---
cyclopropenone	21A1	Y	6.87		1	1	1	6.27	8.39	7.25	6.95	7.01	7.06	7.10	7.09	7.14
cyclopropenone	31A1	Y	8.29		1	2	2	8.57	8.94	8.55	8.36	8.53	8.89	---	8.40	8.58
cyclopropenethione	11A2		3.45		1	1	1	3.22	4.29	3.57	3.54	3.44	3.50	3.50	3.53	3.53
cyclopropenethione	11B1		3.42		1	1	1	3.35	5.37	4.20	3.77	3.49	3.61	3.61	3.56	3.56
cyclopropenethione	11B2		4.64		1	1	1	4.33	6.24	5.41	4.95	4.59	4.71	4.71	4.64	4.64
cyclopropenethione	21B2	R	5.21		1	1	1	4.67	5.97	5.71	5.27	5.27	5.32	5.32	5.35	5.35
cyclopropenethione	31B2	R	5.84		1	1	1	5.42	6.87	6.47	5.93	5.96	5.96	5.83	5.76	5.76
methylenecyclopropene	11B2		4.31		1	1	1	3.69	5.41	4.84	4.55	4.25	4.37	4.37	4.30	4.30
methylenecyclopropene	11B1	R	5.35		1	1	1	4.34	5.39	5.57	5.37	5.35	5.36	5.36	5.39	5.37
methylenecyclopropene	11A2	R	5.88		1	1	1	4.67	5.96	6.15	5.90	5.86	5.88	5.88	5.90	5.89
methylenecyclopropene	21A1	Y	6.15		1	1	1	5.42	6.30	6.40	6.18	6.21	6.15	6.18	6.21	6.17
methylenecyclopropene	11A*		3.74		1	1	1	3.16	4.71	3.90	3.90	3.78	3.91	3.91	3.94	3.94
acrolein	21A*	Y	6.70		1	1	2	6.57	7.05	6.85	6.86	6.93	6.91	7.01	6.89	6.92
acrolein	31A*	Y	7.00		1	1	1	6.03	8.77	7.31	7.11	7.01	7.12	7.12	7.15	7.16
butadiene	11Bu		6.27		1	1	1	6.01	6.22	6.25	6.37	6.35	6.35	6.35	6.37	6.37
butadiene	11Bg	R	6.27		1	1	1	5.49	6.19	6.37	6.30	6.33	6.32	6.32	6.35	6.35
butadiene	21Ag	Y	6.59		1	1	1	6.91	7.41	7.31	7.09	7.24	7.19	7.19	7.21	7.17
butadiene	11Au	R	6.59		1	1	1	5.82	6.53	6.68	6.62	6.65	6.65	6.65	6.67	6.67
butadiene	21Au	R	6.74		1	1	1	5.89	6.69	6.88	6.78	6.80	6.80	6.80	6.83	6.83



Molecule	State	Flip	Rydberg	REF	n-CSF			Excitation energy (eV)			ASCC excitation energy (eV)			EOM-CCSD			PLASCC excitation energy (eV)						
					ESMF	CIS	WB97X-V	EOM-CCSD	ESMF	CIS	WB97X-V	EOM-CCSD	ESMF	CIS	WB97X-V	EOM-CCSD							
Medium QUEST set	butadiene	21Bu	Y	R	7.87	1	1	1	7.38	7.83	7.97	7.93	*8.02	*8.01	7.92	7.92	7.93	7.95	7.96	7.94	7.98	7.98	7.97
	glyoxal	11Au			2.90	2	2	1	3.26	3.59	2.85	3.04	3.13	3.13	3.14	--	3.49	3.46	3.46	2.51	2.50	3.04	3.01
	pyrrole	11A2	R		5.14	1	1	1	4.48	5.38	5.54	5.22	5.21	5.21	5.22	5.22	5.24	5.23	5.23	5.24	5.14	5.25	5.26
	pyrrole	21A2	R		5.93	1	1	1	5.19	6.10	6.32	5.99	5.96	5.96	5.92	5.92	6.01	6.02	6.02	6.02	5.99	5.99	6.06
	pyrrole	11B2			6.28	1	1	1	5.80	6.38	6.51	6.37	6.39	6.40	6.37	6.37	6.41	6.40	6.39	6.23	6.30	*6.36	6.35
	pyrrole	11B2			6.28	1	1	1	5.80	6.38	6.51	6.37	6.39	6.40	6.37	6.37	6.41	6.40	6.39	6.23	6.30	*6.36	6.35
	furan	11A2	R		6.00	1	1	1	5.26	6.04	6.26	6.07	6.08	6.08	6.06	6.06	6.12	6.11	6.11	6.12	6.08	6.12	6.14
	furan	11B2			6.39	1	1	1	6.06	6.37	6.52	6.53	6.51	6.51	6.48	6.48	6.52	6.52	6.53	*6.29	6.37	6.44	6.43
	furan	11B1	R		6.56	1	1	1	5.68	6.54	6.80	6.61	6.62	6.62	6.61	6.61	6.66	6.66	6.66	6.68	6.64	6.64	6.70
	furan	21A2	R		6.74	1	1	1	5.91	6.81	7.06	6.80	6.78	6.78	6.76	6.76	6.81	6.81	6.83	6.85	6.79	6.76	*6.87
	furan	21B2	R		7.40	1	1	1	6.84	7.42	7.63	7.47	--	--	--	--	--	--	--	7.47	7.46	7.53	7.53
	cyclopentadiene	11B2			5.60	1	1	1	5.33	5.50	5.58	5.71	5.67	5.67	5.67	5.70	5.70	5.68	5.69	5.59	5.59	5.61	5.59
	cyclopentadiene	11A2	R		5.70	1	1	1	4.90	5.71	5.91	5.74	5.78	5.78	5.77	5.77	5.80	5.80	5.79	5.83	5.79	5.85	5.84
	cyclopentadiene	11B1			6.34	1	1	1	5.37	6.27	6.54	6.36	6.39	6.39	6.39	6.39	6.42	6.42	6.41	6.41	6.44	6.44	6.47
	cyclopentadiene	21A2	R		6.39	1	1	1	5.50	6.43	6.67	6.42	6.43	6.43	6.41	6.41	6.46	6.45	6.45	6.51	6.47	6.52	6.52
	cyclopentadiene	21B2	R		6.55	1	1	1	5.64	6.53	6.74	6.58	6.37	6.37	6.58	6.58	--	6.58	6.57	6.65	6.65	6.68	6.67
	thiophene	11B2			6.06	1	1	1	5.90	6.06	6.16	6.20	6.22	6.22	6.20	6.20	6.25	6.24	6.23	6.08	6.06	6.10	6.09
	thiophene	11A2	R		6.06	1	1	1	5.46	6.27	6.44	6.13	6.17	6.17	6.16	6.16	6.19	6.19	6.19	6.19	6.16	6.21	6.21
	thiophene	11B1			6.17	1	2	1	5.76	6.62	6.59	6.31	6.40	6.40	--	--	6.35	6.35	6.36	5.75	--	6.30	*6.37
	thiophene	21A2			6.31	1	1	1	6.37	6.73	6.56	6.37	6.44	6.44	6.45	6.45	6.49	6.46	6.46	6.22	6.29	6.41	6.41
	thiophene	21B2	R		7.44	1	1	2	6.96	7.69	7.77	7.52	7.56	7.56	7.54	7.54	--	7.58	7.58	7.59	7.59	7.51	--
	imidazole	11A*			5.60	1	1	1	4.84	5.84	5.98	5.68	5.65	5.65	5.66	5.66	5.69	5.68	5.68	5.68	5.55	5.55	5.68
	imidazole	21A*	Y		6.43	1	1	1	6.04	6.73	6.76	6.58	6.56	6.68	6.66	6.66	6.53	6.72	6.68	5.98	6.44	6.84	6.93
	imidazole	21A*			6.42	1	1	1	5.53	6.49	6.72	6.47	6.40	6.40	6.34	6.34	6.46	6.46	6.47	6.49	6.49	6.45	6.53
	benzene	11E1g	R		6.46	1	1	1	5.89	6.60	6.83	6.49	6.58	6.58	6.56	6.56	6.60	6.60	6.59	6.58	6.58	6.62	6.61
	tetrazine	11B3u			2.50	1	1	1	3.33	3.53	2.66	2.65	3.03	3.03	3.03	3.03	3.09	3.05	3.05	2.69	2.68	2.75	2.70
tetrazine	11Au			3.70	1	1	1	5.31	5.63	4.00	3.93	4.38	4.38	4.37	4.37	4.44	4.42	4.42	3.97	3.93	4.02	3.98	
tetrazine	11B2g			5.50	1	2	1	6.64	6.79	5.98	5.88	6.40	6.40	--	--	6.46	6.46	6.41	5.54	5.54	--	5.57	
pyridazine	11B1			3.86	1	1	1	4.30	4.95	4.07	4.04	4.16	4.16	4.24	4.24	4.25	4.25	4.22	3.92	3.81	3.93	3.90	
pyridazine	11B2	R		6.06	1	1	3	6.55	8.44	6.76	6.25	6.37	6.37	6.44	6.44	--	--	6.42	6.26	*5.78	--	6.24	
pyridazine	21B1			6.41	1	1	1	7.48	8.40	6.69	6.66	6.91	6.91	7.01	7.01	7.01	6.98	6.98	6.60	6.80	6.62	6.60	
cynoacetylene	11sig-	(a)5.91			2	2	2	5.02	5.13	5.28	6.00	6.19	6.19	6.20	6.20	6.22	6.22	6.20	6.19	6.19	6.08	6.13	
cynoacetylene	11del	(a)6.17			2	2	2	5.31	5.42	5.50	6.25	6.55	6.55	6.56	6.56	6.58	6.58	6.56	6.52	6.52	6.41	6.46	
cyanogen	11sigu-	(a)6.51			2	2	2	5.43	5.54	6.09	6.63	6.84	6.84	6.85	6.85	6.87	--	6.85	6.58	*6.49	*6.47	*6.58	
cyanogen	11delu	(a)6.77			2	2	2	5.78	5.88	6.08	6.89	7.22	7.22	7.23	7.23	7.26	--	7.24	6.95	6.95	6.93	6.97	
diacetylene	11sigu-	(a)5.43			2	2	2	4.68	4.77	4.86	5.51	5.71	5.71	5.71	5.71	5.73	5.73	5.72	5.60	5.57	5.61	5.59	
diacetylene	11delu	(a)5.69			2	2	2	4.94	5.02	5.04	5.75	6.06	6.06	6.06	6.06	6.08	6.07	6.07	--	--	--	--	
pyrazine	11B3u	4.19			1	1	1	4.94	5.15	4.36	4.35	4.70	4.70	4.71	4.71	4.75	4.75	4.72	4.32	4.32	4.33	4.38	
pyrazine	11Au	4.98			1	1	1	6.53	6.95	5.20	5.19	5.54	5.54	5.55	5.55	5.59	5.57	5.57	5.18	5.18	5.15	5.22	
pyrazine	21Ag	6.53	Y	R	1	1	1	7.64	8.49	7.09	6.66	7.04	7.04	7.02	7.08	7.09	7.06	7.07	6.82	6.81	6.76	6.85	
pyrazine	11B1g	6.75			1	1	1	8.67	9.72	7.20	7.10	7.43	7.43	7.41	7.41	7.47	7.47	7.47	6.95	6.95	*6.90	6.98	
pyrazine	21B1g	R		7.14	1	1	1	6.40	7.07	7.42	7.17	7.20	7.20	7.18	7.18	7.24	7.24	7.22	7.24	7.24	7.22	7.29	
pyrazine	21B2u	R		7.13	1	2	1	8.17	9.14	7.76	7.27	7.61	7.61	--	--	7.66	7.66	7.64	7.41	7.41	--	7.43	
pyridine	11B1	5.00			1	1	1	4.73	6.16	5.26	5.19	5.10	5.10	5.25	5.25	5.27	5.27	5.26	5.01	5.01	4.82	4.92	
pyridine	11A2	5.41			1	1	1	5.62	7.37	5.64	5.61	5.63	5.63	5.75	5.75	5.72	5.71	5.71	5.46	5.46	5.41	5.45	

Molecule	State	Flip	Rydberg	REF	n-CSF			Excitation energy (eV)			ASCC excitation energy (eV)			EOM-CCSD			PLASCC excitation energy (eV)		
					ESMF	CIS	WB97X-V	ESMF	CIS	WB97X-V	ESMF	CIS	WB97X-V	ESMF	CIS	WB97X-V	ESMF	CIS	WB97X-V
pyridine	21A2		R		1	1	1	6.08	6.79	7.08	6.78	6.83	6.82	6.82	6.85	6.87	6.85	6.83	6.89
	11B1				1	1	1	5.19	5.90	4.75	4.66	4.88	4.94	4.94	4.97	4.99	4.97	4.63	4.56
	11A2				1	1	1	5.88	6.56	5.10	5.06	5.35	5.39	5.39	5.40	5.43	5.40	5.03	5.05
	21B1				1	2	1	7.72	8.24	6.54	6.52	6.87	6.87	---	6.96	6.96	6.93	6.46	6.51
	21B2		R		1	1	1	7.33	8.58	7.21	6.72	7.03	7.07	7.11	7.11	7.07	7.07	6.86	*6.83
triazine	11E'				1	1	1	7.86	9.07	7.70	7.29	7.63	7.63	7.63	7.68	7.69	7.68	7.44	7.50
Charge transfer set	ammonia-difluorine	21A1			1	1	1	7.51	11.38	6.30	9.54	9.17	9.16	9.13	9.14	9.14	9.20	9.37	9.34
	acetone-difluorine	31A*			1	1	1	4.17	8.72	3.70	6.28	5.74	5.77	5.77	5.74	5.74	5.84	5.85	5.81
	pyrazine-difluorine	21B2			1	1	1	6.42	9.26	4.35	6.77	6.51	6.42	6.42	6.48	6.48	6.56	6.47	6.43
	pyrazine-difluorine	21A2			1	1	1	4.83	7.37	4.41	6.73	6.41	6.41	6.36	6.37	6.37	6.72	6.58	6.62
	ammonia_oxygendifluoride	41A'	Y		1	2	1	5.41	9.61	5.11	7.33	6.95	6.92	7.56	7.57	6.95	7.08	7.01	6.97
	tetrafluoroethylene-ethylene	51B1			1	1	1	10.53	12.34	9.48	10.87	10.39	10.39	10.55	10.55	10.31	10.69	10.58	10.57
	3,5-difluoro-penta-2,4-dienamine	11A"			1	1	1	6.44	8.78	6.68	7.05	6.84	6.84	7.07	7.07	6.98	6.96	6.76	6.82
																			6.74